Visualization and quantification of two-phase flow in transparent miniature packed beds

Peixi Zhu and Kyriakos D. Papadopoulos

Phys. Rev. E **86**, 046313 — Published 16 October 2012

DOI: 10.1103/PhysRevE.86.046313

Visualization and quantification of two-phase flow in transparent miniature packed beds

Peixi Zhu* and Kyriakos D. Papadopoulos†

Department of Chemical and Biomolecular Engineering,

Tulane University, New Orleans, Louisiana, 70118, USA

Abstract

Optical microscopy was used to visualize the flow of two phases (BP oil and an aqueous surfactant phase) in confined space, three-dimensional, transparent, natural porous media. The porous media consisted of water-wet cryolite grains packed inside cylindrical, glass micro-channels, thus producing microscopic packed beds. Primary drainage of BP oil displacing an aqueous surfactant phase was studied at capillary numbers that varied between 10^{-6} and 10^{-2}. The confinement space had a significant effect on the flow behavior. Phenomena of burst motion and capillary fingering were observed for low capillary numbers due to the domination of capillary forces. It was discovered that breakthrough time and capillary number bear a log–log scale linear relationship, based on which a generalized correlation between oil travel distance x and time t was found empirically.

* zpeixi@tulane.edu

† kyriakos@tulane.edu

I. INTRODUCTION

The explosion of the Deepwater Horizon operated by British Petroleum caused a serious oil spill disaster that threatened the environment of costal area near the Gulf of Mexico. It is known that although the surface of contaminated geological sediment can eventually be cleaned, the oil that penetrates underground can persist for decades [1]. With physical force, such as precipitation, underground flow, sea waves or tides, trapped oil can be mobilized. When that happens, it involves movement of multiphase fluid in porous media. Understanding such phenomenon has significant value also in a number of practical applications, such as oil recovery, hydrology, non-aqueous phase liquid (NAPL) contamination, fuel cell technology [2, 3] and transport in the cardiovascular system [4].

In some cases, fluid that initially occupies pore space is replaced by another immiscible fluid that can coexist with the former. This process is known as displacement, and has been studied largely in the past few decades due to its importance to reservoir engineering, hydrology, agricultural irrigation and treatment of ground water contamination [5–17]. One of the interesting topics is the mobilization of the invading fluid interface, which is hard to predict in porous media of geological sediment, such as sand, soil and rock. The frontal dynamics can affect the oil recovery efficiency, as well as mass transport between NAPL/aqueous interface. The frontal structure can vary from compact to fingering pattern, depending on capillary number and viscosity ratio between invading and defending fluid [11, 15, 18, 19]. In particular, at low injection rate, where viscous force can be neglected and capillary force dominates, capillary fingering is manifested. Fingering pattern produces pockets of defending fluid, which leads to reduction of displacement efficiency.

In this work, we focus on the displacement of a surfactant aqueous phase by oil phase. Such process is known as drainage, where a wetting fluid is displaced by non-wetting fluid. The opposite case, where the invading phase is non-wetting fluid, is termed imbibition [20]. At low capillary number, their displacement mechanisms are quite different; in imbibition, displacement takes place at the narrowest pore spontaneously, while in drainage, displacement occurs when the capillary pressure at pore scale level exceeds a certain threshold. Such pressure threshold is given by the equilibrium capillary pressure at the minimum pore width [21] and can be calculated from Young-Laplace equation. An important characteristic of capillary dominated drainage is the discontinuous burst-like flow motion, known as Haines

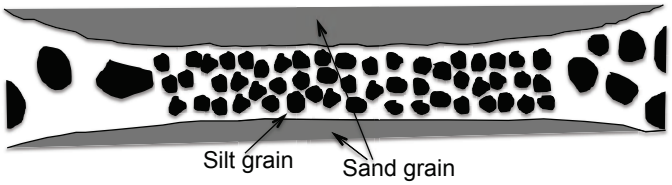

FIG. 1. A scheme of silt grain particles between sand grains.

Jump [22].

In some geological areas, sediments are composed of more than one type of soil textures, e.g., a sand loam or silt loam. In the Gulf of Mexico, this can occur in the transition region from one type of soil sediment to another [23]. The heterogeneity of such soil mixtures can lower the porosity of the sediment because of non-uniform distribution of grain size, since small grains can fill the interstitial pore channel between large grains. In addition, differences in wettability among different soil textures introduce more complexity to the transport of oil in pore spaces. A scenario is given in Fig. 1, in which a micro-channel pore space between sand grains is filled by smaller silt grain particles. The available pore space that allows fluid to pass through is significantly reduced and so is the local porosity. When the spilled oil invades such micro-channels, the shear force from a subsequent imbibition due to water precipitation or tidal water movement can lead to tiny, trapped oil clusters. In general, sand's wettability by water is different than that of silt. As a result, the capillary resistance that corresponds to these two soil materials is not the same. Therefore, two-phase flow behavior can be different than that in homogeneous soil textures, especially when the capillary number is low and capillary resistance dominates the system, and knowing flow behavior in a single micro-channel pore may help understand two-phase flow at large-scale heterogeneous porous media.

Here, we are presenting experiments of primary drainage displacement conducted in a microscopic cylindrical packed bed, which has random and transparent packing. Such porous-media geometry was made in order to investigate two-phase flow in heterogeneous soil texture, where smaller grains fill the micro-channels, as depicted in Fig. 1. It should be noted that previous studies have used x-ray computed tomography on cylindrical-shaped tubes packed with random natural porous media [24–26], whereas in our experiments, real-time films of two-phase flow in a porous-medium packed bed were produced through optical-video microscopy. The grains were packed in a cylindrical glass channel that was less than 100 μm

in diameter and grain size was a few times smaller than the host channel's diameter. In such case, capillary resistance presented by the channel's wall can be significant and as important as the grains of the porous medium. For the fixed total bed length captured by the camera, we studied the effect of capillary number on the x-vs.-t behavior of the displacing oil phase, where x is the oil-traveled distance at time t. Capillary number, Ca, is given by

$$\mathrm{Ca} = v\frac{\mu}{\gamma}, \tag{1}$$

where v is superficial linear flow rate, μ is viscosity of the more viscous fluid and γ is interfacial tension between wetting and non-wetting fluid. BP Deepwater Horizon crude oil was used as the invading fluid and Tween 80 solution, a component of the oil spill dispersant Corexit, was used as the defending fluid. Such combination may model well a practical example of crude oil contamination in geological porous media. By choosing such combination, we wish to extract the fundamental behavior of two-phase flow in confined geometries that may be useful in our overall effect to contribute to the understanding of how oil-spill that has been trapped in porous media may be mobilized. In addition, BP crude oil, a Louisiana sweet crude, provides a contrast color to the aqueous phase and has low viscosity. The porous medium was made of particles of cryolite, which has a refractive index close to that of water and henceforth is visible when immersed by water. We found that the breakthrough time of the invading fluid and capillary number Ca have a power law relationship that deviates from two-phase flow in a cylindrical tube in the absence of porous medium. It is valid at least for medium-to-low flow rate, that is, capillary numbers between 10^{-2} and 10^{-6}. To our knowledge, few people have investigated the correlation between capillary number and breakthrough time for two-phase flow [16]. Furthermore, we were able to find a generalized and empirical correlation between the oil phase travel distance x and time t. Ferer *et al.* have studied how the non-wetting phase moves as a function of time for two-phase drainage in 2-dimensional network structure [14, 19, 27, 28]. In this paper, the results were obtained from cylindrical micro-channels of approximately 90 μm in diameter and with a very narrow diameter-size distribution. The exact correlation may or may not apply to non-cylindrical channels or to channels of different diameters. Further investigation is needed to discover how channel geometry and size may affect flow behavior. However, we claim to be the first to discover that a correlation exists between x and t for a cylindrical, packed, micro-channel geometry.

II. EXPERIMENT

A. Materials

Polyoxyethylene sorbitan monooleate (Tween® 80) and cryolite mineral particles (Na_3AlF_6, 97% purity) were purchased from Sigma-Aldrich. Prior to usage, cryolite was sieved in deionized water so that the average particle diameter was around 30–40 μm. Particles were then placed in oven at 70 °C to remove water, followed by immersion in a 10^{-4} mol/L Tween 80 aqueous solution. Crude oil sample came directly from BP.

B. Cylindrical micro-channels

Our lab has developed and used a video-capillary-microscopy technique for the study of several phenomena that happen in the confined space of cylindrical channels, including transport of bacterial migration [29–31], electrokinetic flows [32, 33] and reaction of levitated drops with a levitating fluid [34]. In the present paper, such glass micro-channels were filled with cryolite particles. The channels were centrally pulled from PYREX® melting-point tubes (1.5–1.8 mm O.D. × 100 mm × 0.2 mm wall) by heating and pulling on a vertical micropipette puller (Narishige, PB-7) until the I.D. of the middle of the tube was reduced to around 90 μm. Subsequent experiments and observations were conducted in this thin part, referred to as cylindrical micro-channel (Fig. 2(a)).

C. Physicochemical properties

Interfacial tension between crude oil and 10^{-4} mol/L Tween 80 solution was measured on a tensiometer (ramé-hart instrument co., NJ). Interfacial tensions of crude oil/air and Tween 80 solution/air were also measured for the purpose of calculating contact angle.

The Young equation was used to obtain contact angle for the glass/Tween 80 solution/crude oil system. First, the contact angle of a Tween 80 solution droplet on glass and that of an oil droplet on glass were measured via the sessile drop method and using the same equipment as above. In both cases the surrounding fluid was air. Using the values of the interfacial tension of Tween 80 solution/crude oil, Tween 80 solution/air and crude oil/air, the Young equation was written for the systems glass/Tween 80 solution/crude oil,

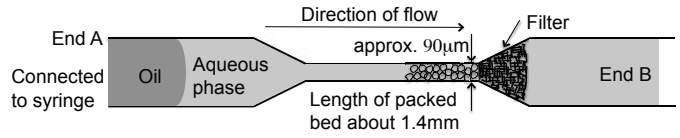

(a)

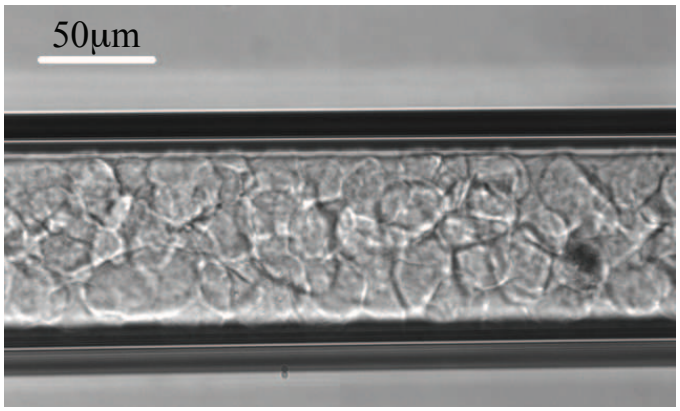

(b)

FIG. 2. (a) Scheme of micro-channel packed bed. (b) Snapshot of cryolite particles inside the channel.

glass/Tween 80 solution/air and glass/crude oil/air, and so the contact angle of Tween 80 solution on glass in crude oil could be calculated.

Since the cryolite that constitutes the porous medium is in powder form, the sessile drop method cannot be used to measure cryolite contact angles for the two liquids. To circumvent that, our attempts included using a flat cryolite stone and a cryolite-porous-medium column that employed the Washburn method. The results were not reliable and thus are not presented here. However, from our video microscopy visualization, we are convinced that crude oil is the non-wetting phase to the cryolite grains and Tween 80 solution is the wetting phase. The evidence is that when small amount of crude oil was injected into the cryolite porous media filled with Tween 80 solution, the oil phase broke into clusters or droplets rather than spreading onto the particle surface.

Viscosity of crude oil was determined on a rheometer (TA Instruments, DE). All physicochemical constants of the system are summarized in Table I.

TABLE I. Physicochemical properties of the glass/Tween 80 solution/crude oil system.

Notation	Unit	Value
γ [a]	mN/m	14.0
θ_{glass} [b]	degrees	15
θ_{cryolite} [c]	degrees	N/A [d]
μ [e]	mPa · s	3.50

[a] γ : Tween 80 solution/crude oil interfacial tension.
[b] θ_{glass} : Contact angle of Tween 80 solution on glass in crude oil.
[c] θ_{cryolite} : Contact angle of Tween 80 solution on cryolite in crude oil.
[d] No experimental data available. Microscopic visualization indicates that Tween 80 solution wets the cryolite grains.
[e] μ : Crude oil viscosity.

D. Drainage displacement

Cryolite particles were sucked from one end of the tube (End A) together with Tween 80 solution until the length of porous medium inside the micro-channel was around 1.4 mm. KimWipes$^{\text{TM}}$ paper was used to plug the other end of the tube (End B), so as not to allow the cryolite packing to escape from the narrow section of the channel towards the larger diameter of the tube. Using suction on the side of the tube that had the plugging, a suspension of cryolite particles was introduced from tube End A, leading to the formation of a porous-medium column (Fig. 2(a)). After a desired amount of cryolite was piled up inside the micro-channel so as to form an aqueous-surfactant solution filled packed bed, the whole channel was placed on a tube holder. Subsequently, End A of the glass tube was connected to a 1 ml syringe (Hamilton Company) through ethyl vinyl acetate tubing (Cole-Parmer, 0.51 mm I.D.). BP oil was then injected through the syringe to displace the aqueous phase. The injection was controlled via a syringe pump (Harvard Apparatus Picoplus). Since μ

and γ are unchanged in the system, the capillary number was changed only through v. This was done by monitoring the flow rate via the syringe pump. For each capillary number, a freshly made porous-medium packed bed was used to conduct experiment of drainage displacement. This ensured that, for each Ca, the packing of a given porous medium was randomly different than the others.

E. Video microscopy

The displacement process was observed over an inverted microscope (Olympus IMT-2) with a $4\times$ magnification objective. The packing's cryolite particles were transparent and visible inside the micro-channels through their dark contours (Fig. 2(b)), and the displacement of oil that advanced through the random pores could be clearly seen. The advancement of the oil phase from one end of the camera's viewing field to the other was recorded by a high-frame-rate digital camera (Imperx IPX-VGA-210-L) via an interactive software (Xcap). For $\mathrm{Ca} > 10^{-3}$, displacement processes were captured with at least 150fps. For others, a frame rate of 24fps was used. Videos were saved for further analysis.

III. RESULTS AND DISCUSSION

A. Visualization of flow pattern

Snapshots of injected oil invading water are shown in Fig. 3 for capillary number $\mathrm{Ca} = 5.67 \times 10^{-5}$. In the second frame, it can be clearly observed that the interface is not flat, but rather a wide, irregular fingering structure, with pockets of defending fluid left behind. Such phenomena, known as capillary fingering, are quite similar to two-phase flow in large-scale porous media, where geometrical confinement is not present. The pockets were replaced by the oil phase at a later stage (Fig. 3, third frame from top). Fingering structures were also observed for Ca on the order of 10^{-4}, although the height was shorter. It was also observed that the capillary fingering could propagate backward and laterally to a certain extent, even though the invasion of the crude oil and the glass wall limited such propagation. According to these results, when geological micro-channels are invaded by crude oil at low Ca, the flow can exhibit capillary fingering with thin width, e.g., less than 50 μm.

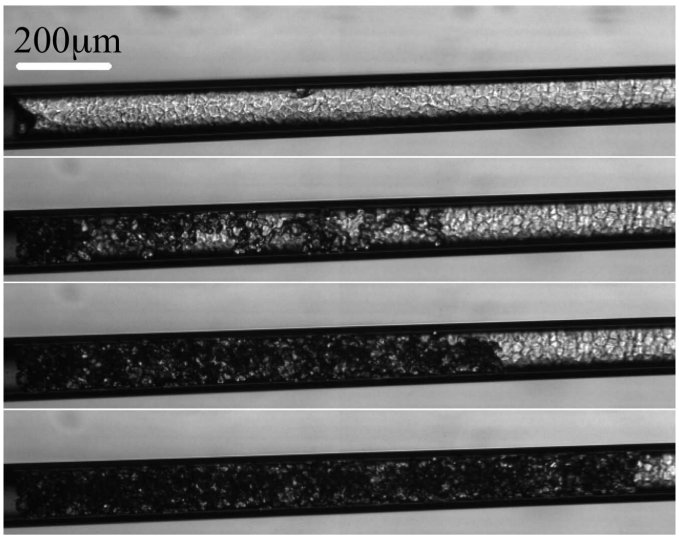

FIG. 3. From top to bottom, snapshots of displacement process for Ca $= 5.67 \times 10^{-5}$ at time $t = 0$ s, 101.4 s, 113.5 s and 129.3 s (near breakthrough). The dark phase is oil, while the bright phase is Tween 80 aqueous solution. Flow direction is from left to right.

When capillary number was increased to the order of 10^{-3}, the front of the oil phase looked more stable and fingering structure was not seen clearly (Fig. 4). Considering that the viscosity ratio between the invading fluid (crude oil) and defending fluid (Tween 80 solution) is greater than 1, these images show the change of flow pattern from capillary fingering to compact flow, which was predicted in the simulations of Ferer *et al.* [27]. Surprisingly, fingering structures were not observed when Ca came down to the order of 10^{-6} (Fig. 5), although pockets of the defending fluid were formed during the displacement process. In our long, narrow micro-channel system, the sheer number of fractals can make them collapse into a frontal interface that appears smooth, while in fact it may consist of a number of merged fingers. This reasoning of wall effect has actually been put forward by Ferer *et al.*, in justifying the use of a wide-and-short porous medium geometry in their calculations [14, 19].

B. Measurement of oil travel distance

For all experiments, the history of each biphasic interface travel distance is presented in Fig. 6. The plot was normalized for the purpose of comparison among different capillary numbers. The distance and time are normalized by the total observed length L, and the breakthrough time t_{b}, respectively. Here t_{b} is defined as the amount of time it takes for the

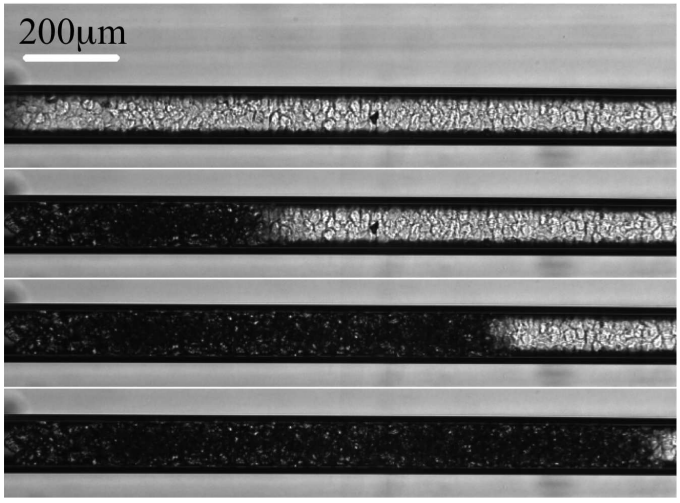

FIG. 4. From top to bottom, snapshots of displacement process for Ca $= 5.06 \times 10^{-3}$ at time $t = 0$ s, 0.02 s, 0.051 s and 0.07 s (near breakthrough). The dark phase is oil, while the bright phase is Tween 80 aqueous solution. Flow direction is from left to right.

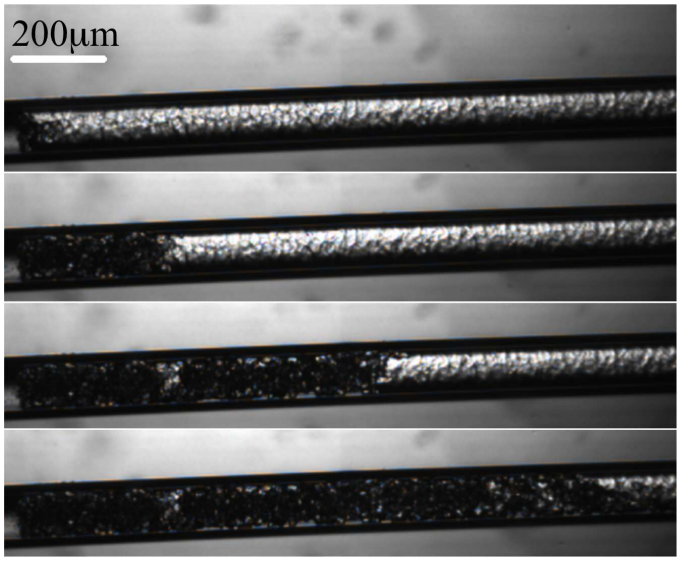

FIG. 5. From top to bottom, snapshots of displacement process for Ca $= 5.62 \times 10^{-6}$ at time $t = 0$ s, 801 s, 1246 s and 1505 s (near breakthrough). The dark phase is oil, while the bright phase is Tween 80 aqueous solution. Flow direction is from left to right.

front of the oil phase to reach "End B" of the micro-channel (Fig. 2(a)), i.e., the moment of percolation. It was found that the flow behavior of oil phase in such confined geometry was similar to large-scale porous media. For low capillary numbers, e.g., Ca $< 10^{-4}$, the interface advanced discontinuously, i.e., as the front of the interface arrived at a new position,

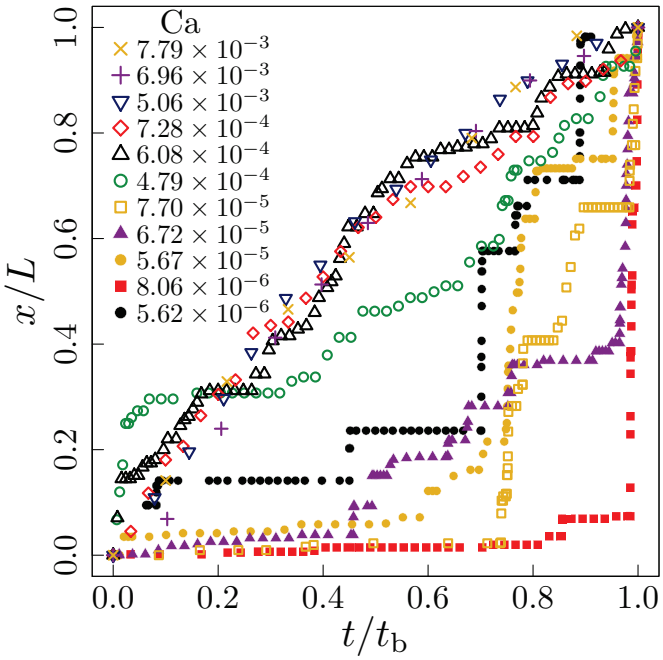

FIG. 6. (Color online) Oil travel distance as a function of time at different capillary numbers. For comparison, the position is normalized by maximum length L, and travel time is normalized by breakthrough time t_{b}.

it tended to stay in that local area for a certain time interval, followed by a sudden invasion, covering a wide distance in a short period of time. This phenomenon, known as burst dynamics [22, 35–37], is the characteristic of drainage displacement. At low Ca, fluid flow is known to be dominated by capillary forces; when oil phase flow meets a local resistance, e.g., a position where the pore space is the narrowest compared to pore spaces in its vicinity, the frontal movement is paused until the pressure that is built overcomes the threshold capillary pressure, which is given by the Young-Laplace equation. The time interval between bursts has been previously studied in two-dimensional flow cells, one of them using glass spheres [21], and the other a lithographically etched, random porous medium [38]. In contrast to those studies that used well-structured two-dimensional porous media, in our experiments the natural porous medium (cryolite) is random, and therefore time intervals between bursts are unpredictable. Fig. 6 also shows that as Ca increased, burst motion gradually diminished and the movement of frontal interface became more continuous, due to the domination of viscous forces over capillary forces.

Breakthrough times of oil phase at different capillary numbers are shown in Fig. 7. Since

the length of packed bed was slightly different for each drainage experiment, a calibrated breakthrough time t_{bc}, given as

$$t_{\mathrm{bc}} = \frac{t_{\mathrm{b}}}{L} L_0, \tag{2}$$

was used to replace t_{b}. The shortest bed length in the experiments was slightly larger than 1400 μm, therefore 1400 μm was chosen as the characteristic length L_0. In other words, we adjusted t_{b} to the breakthrough time that corresponds to position $x = 1400\,\mu\mathrm{m}$. Since L is very close to L_0, t_{bc} is actually nearly equal to t_{b}. For two-phase flow in a cylindrical tube, i.e., second-phase displacement in the absence of a porous medium,

$$t_{\mathrm{b}}\mathrm{Ca} = t_{\mathrm{b}} v \frac{\mu}{\gamma} = L \frac{\mu}{\gamma} = \text{const.},$$

therefore

$$\log_{10} t_{\mathrm{b}} = -\log_{10} \mathrm{Ca} + \text{const.} \tag{3}$$

In plotting t_{bc} vs. Ca on a logarithmic scale, however, it came to our attention that breakthrough time t_{bc} and Ca are correlated by

$$\log_{10} t_{\mathrm{bc}} = -1.54 \log_{10} \mathrm{Ca} - 4.45. \tag{4}$$

Since each of our experiments was conducted on a freshly made micro-channel packed bed, and since each packing of porous media material is completely random, Eq. 4 is a generalized correlation for all capillary numbers and for the sizes of micro-channel and grains we chose. It should be noted that Tallakstad *et al.* in a system that used a flow mixture of wetting and non-wetting fluid to displace air, also measured the relation between breakthrough time and capillary number for flow in porous medium in a $85 \times 42\,\mathrm{cm}^2$ two-dimensional square channel [16] and found log–log correlation that had a slope of -0.89. Our system differs in many aspects from theirs, most notably in that flow was generated in a micro-channel packed bed where primary drainage was manifested. The deviation of slope from -1 in Eq. 4 is probably due to the expected capillary resistance in porous media. In addition, the glass wall that confines the porous medium may also affect the coefficients in Eq. 4. As stated earlier in the experimental section, both the glass wall and the cryolite grains are wettable by the aqueous phase. However, the degree of wettability is likely to be different for the two substrates. As a result, the capillary resistances to the invading phase should be different and may also play a role in the deviation from the negative-one slope.

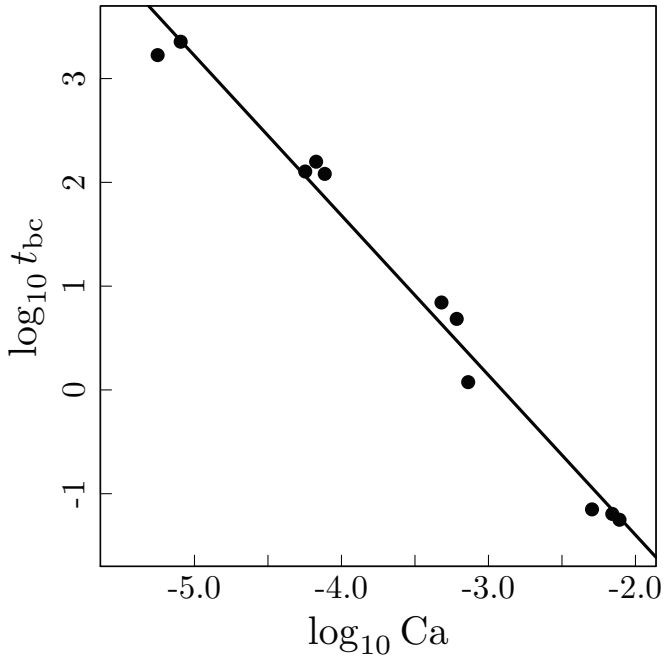

FIG. 7. Breakthrough time as a function of capillary number Ca. $t_{\rm bc}$, the calibrated breakthrough time that has the unit of second, is defined as $t_{\rm bc} = t_{\rm b}/L * L_0$, where L_0 is equal to 1400 μm.

One of our interests was finding how the oil's travel distance, x, correlates with time. Inspired by Eq. 4, we sought and found the empirical correlation $\log_{10} \frac{x}{\left(t\mathrm{Ca}^{1.54}\right)^7}$ vs. $\log_{10}\left(t\mathrm{Ca}^{1.54}\right)$. Presenting all experimental results on a log–log plot in Fig. 8, it can be seen that the reduced x-vs.-t data fall onto the green(lighter grey)-shaded linear region, the centerline of which is $Y = 4.60 - 6.45X$. For $\mathrm{Ca} > 10^{-4}$, all data collapse onto a linear curve $Y = 5.54 - 6.45X$. For $\mathrm{Ca} < 10^{-4}$, the curves show zigzag shape due to burst motion, but also collapse at final stage. According to Fig. 8, oil travel distance x for $\mathrm{Ca} > 10^{-4}$, or for $\mathrm{Ca} < 10^{-4}$ at large time scale, can be written as

$$x = \mathrm{const}\left(t\mathrm{Ca}^{1.54}\right)^{0.55}, \tag{5}$$

or

$$x \propto \left(t^{0.55}\right)\left(\mathrm{Ca}^{0.847}\right). \tag{6}$$

So, in our 3D micro-channel geometry, x scales as the power of 0.55 in t and 0.847 in capillary number. Although this is a crude prediction of the history of biphasic interface, we believe that it is a generalized correlation for the x-vs.-t behavior of displacement of Tween 80 solution by a crude-oil phase in micro-channel-confined porous media with the

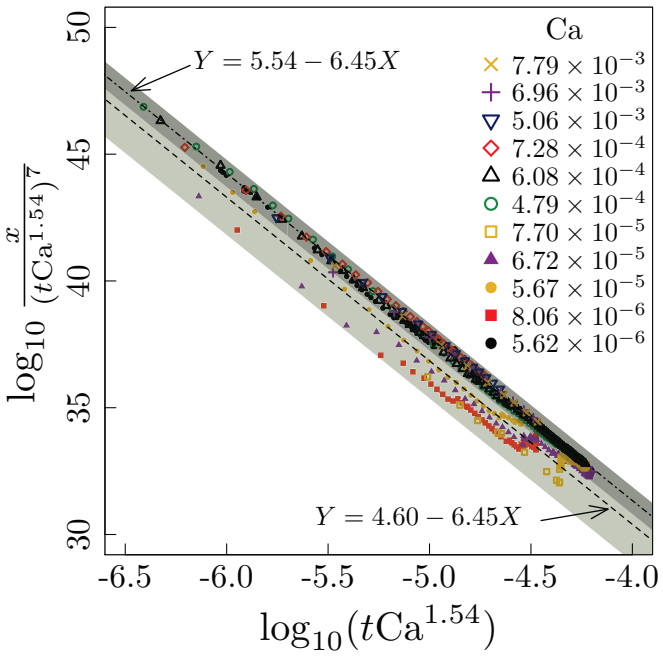

FIG. 8. (Color online) A plot of $\log_{10} \frac{x}{(t\mathrm{Ca}^{1.54})^7}$ against $\log_{10}(t\mathrm{Ca}^{1.54})$ for all capillary numbers. $\frac{x}{(t\mathrm{Ca}^{1.54})^7}$ is in $\mu\mathrm{m/s}^7$ and $t\mathrm{Ca}^{1.54}$ is in second. All data fall into the green (lighter grey) straight-line region, the center of which is represented by the dotted line. In addition, the grey (darker grey) region, with the dash dotted line as the center, is the area where all data for $\mathrm{Ca} > 10^{-4}$ collapse.

chosen diameter. The micro-channel size effect on the flow behavior is not considered in the present work. It is possible that the correlation in Fig. 8 will not apply to micro-channels with different diameters. In practical crude oil/aqueous/soils micro-channel systems, such correlation also may not hold since the wetting properties of the larger soil grains that form the micro-channel and finer grains that fill the channel pores can be different than the wetting properties of the glass wall and cryolite grains in our system. However, we may draw an analogy to the classic Blake-Kozeny equation that predicts one-phase flow through a porous medium based on knowledge of the flow in empty cylindrical tubes (Hagen-Poiseuille) that allegedly constitute the porous medium. Accordingly, understanding micro-channel, two-phase, porous-media flow, may be a step towards the better prediction of two-phase flow in porous media that are composed of micro-channels. Ultimately, it should also be possible to predict two-phase flow in a macroscopic porous medium, the micro-channels of which are packed with finer-grain particles, based on the knowledge of two-phase flow behavior in a fine-particle-packed micro-channel.

IV. CONCLUSIONS

Two-phase primary drainage flow experiments were conducted in micro-channel beds of transparent, natural porous media through optical microscopy, which showed a restrain of capillary fingering propagation at low capillary number. Much like large-scale porous media, capillary fingerings were observed at early stage of displacement for small Ca, and coarsened into compact pattern as oil phase was invading a Tween 80 aqueous phase. Comparison of the history of non-wetting phase travel distance for various capillary numbers revealed burst dynamics at Ca $< 10^{-4}$ and continuous movement for large Ca. The logarithmic plot of Ca vs. t_{bc} in Fig. 7 showed that breakthrough time is proportional to $\mathrm{Ca}^{-1.54}$, which differs from two-phase flow in a cylindrical tube in the absence of porous medium. Furthermore, a generalized empirical correlation exists between x and t for all investigated capillary numbers. Such correlation tells us that, for our system of micro-channel geometry, x scales as 0.55 power of displacement time and 0.847 of capillary number.

ACKNOWLEDGMENTS

We acknowledge partial support from NSF CBET (Award number 1052697) and from the Gulf of Mexico Research Initiative.

[1] L. Guterman, Science **323**, 1558 (2009).

[2] J. H. Kang, K.-J. Lee, J. H. Nam, C.-J. Kim, H. S. Park, S. Lee, and I. Kwang, J. Power Sources **195**, 2608 (2010).

[3] J. H. Kang, K. N. Kim, J. H. Nam, and C.-J. Kim, Int. J. Hydrogen Energy **37**, 1642 (2012).

[4] Z. J. Huang and J. M. Tarbell, Am. J. Physiol. **273**, H464 (1997).

[5] A. C. Payatakes, K. M. Ng, and R. W. Flumerfelt, AIChE J. **26**, 430 (1980).

[6] R. Lenormand, C. Zarcone, and A. Sarr, J. Fluid Mech. **135**, 337 (1983).

[7] D. Wilkinson and J. F. Willemsen, J. Phys. A: Math. Gen. **16**, 3365 (1983).

[8] J.-D. Chen and J. Koplik, J. Colloid Interface Sci. **108**, 304 (1985).

[9] M. M. Dias and A. C. Payatakes, J. Fluid Mech. **164**, 337 (1986).

[10] D. Wilkinson, Phys. Rev. A: At., Mol., Opt. Phys. **34**, 1380 (1986).

[11] M. Ferer, R. A. Geisbrecht, W. N. Sams, and D. H. Smith, Phys. Rev. A: At., Mol., Opt. Phys. **45**, R6973 (1992).

[12] O. I. Frette, K. J. Måløy, J. Schmittbuhl, and A. Hansen, Phys. Rev. E: Stat., Nonlinear, Soft Matter Phys. **55**, 2969 (1997).

[13] E. Aker, K. J. Måløy, and A. Hansen, Phys. Rev. E: Stat., Nonlinear, Soft Matter Phys. **61**, 2936 (2000).

[14] M. Ferer, G. S. Bromhal, and D. H. Smith, Phys. Rev. E: Stat., Nonlinear, Soft Matter Phys. **67**, 051601 (2003).

[15] M. Ferer, C. Ji, G. S. Bromhal, J. Cook, G. Ahmadi, and D. H. Smith, Phys. Rev. E: Stat., Nonlinear, Soft Matter Phys. **70**, 016303 (2004).

[16] K. T. Tallakstad, G. Løvoll, H. A. Knudsen, T. Ramstad, E. G. Flekkøy, and K. J. Måløy, Phys. Rev. E: Stat., Nonlinear, Soft Matter Phys. **80**, 036308 (2009).

[17] S. A. Bowden, J. M. Cooper, F. Greub, D. Tambo, and A. Hurst, Lab Chip **10**, 819 (2010).

[18] M. M. Dias and A. C. Payatakes, J. Fluid Mech. **164**, 305 (1986).

[19] M. Ferer, G. S. Bromhal, and D. H. Smith, Phys. Rev. E: Stat., Nonlinear, Soft Matter Phys. **76**, 046304 (2007).

[20] R. Lenormand, J. Phys.: Condens. Matter **2**, SA79 (1990).

[21] L. Furuberg, K. J. Måløy, and J. Feder, Phys. Rev. E: Stat., Nonlinear, Soft Matter Phys. **53**, 966 (1996).

[22] W. B. Haines, J. Agric. Sci. **20**, 97 (1930).

[23] G. Y. Kim, M. D. Richardson, D. L. Bibee, D. C. Kim, R. H. Wilkens, S. R. Shin, and S. T. Song, Geosci. J. **8**, 95 (2004).

[24] K. A. Culligan, D. Wildenschild, B. S. B. Christensen, W. G. Gray, and M. L. Rivers, Adv. Water Resour. **29**, 227 (2006).

[25] G. Schnaar and M. L. Brusseau, Vadose Zone J. **5**, 641 (2006).

[26] D. A. DiCarlo, L. D. Seale, K. Ham, and C. S. Willson, Adv. Water Resour. **33**, 485 (2010).

[27] M. Ferer, G. S. Bromhal, and D. H. Smith, Phys. Rev. E: Stat., Nonlinear, Soft Matter Phys. **71**, 026303 (2005).

[28] M. Ferer, G. S. Bromhal, and D. H. Smith, Adv. Water Resour. **30**, 284 (2007).

[29] Z. Liu and K. D. Papadopoulos, Appl. Environ. Microbiol. **61**, 3567 (1995).

[30] Z. Liu and K. D. Papadopoulos, Biotechnol. Bioeng. **51**, 120 (1996).

[31] Z. Liu, W. Chen, and K. D. Papadopoulos, Biotechnol. Bioeng. **53**, 238 (1997).

[32] C.-C. Kuo and K. D. Papadopoulos, Environ. Sci. Technol. **30**, 1176 (1996).

[33] Z. Liu, W. Chen, and K. D. Papadopoulos, Environ. Microbiol. **1**, 99 (1999).

[34] M. Garcia-Bermudes, R. Rausa, and K. Papadopoulos, Ind. Eng. Chem. Res. **50**, 14142 (2011).

[35] L. Furuberg, J. Feder, A. Aharony, and T. Jøssang, Phys. Rev. Lett. **61**, 2117 (1988).

[36] K. J. Måløy, L. Furuberg, J. Feder, and T. Jøssang, Phys. Rev. Lett. **68**, 2161 (1992).

[37] E. Aker, K. J. Måløy, A. Hansen, and S. Basak, Europhys. Lett. **51**, 55 (2000).

[38] D. Crandall, G. Ahmadi, M. Ferer, and D. H. Smith, Physica A (Amsterdam) **388**, 574 (2009).